Lawrence Berkeley National Laboratory
LBL Publications

Title
X-Ray Absorption spectroscopy from H-Passivated Porous Si and Oxidized Si Nanocrystals

Permalink
https://escholarship.org/uc/item/8v64v6zg

Authors
Schuppler, S.
Friedman, S.L.
Marcus, M.A.
et al.

Publication Date
1994-11-01

eScholarship.org Powered by the California Digital Library
University of California

LBL-36911
UC-404

Lawrence Berkeley Laboratory

UNIVERSITY OF CALIFORNIA

Materials Sciences Division

National Center for Electron Microscopy

Presented at the Materials Research Society Symposium,
Boston, MA, November 28–December 2, 1994, and to be
published in the Proceedings

X-Ray Absorption Spectroscopy from H-Passivated Porous Si and Oxidized Si Nanocrystals

S. Schuppler, S.L. Friedman, M.A. Marcus, D.L. Adler,
Y.-H. Xie, F.M. Ross, T.D. Harris, W.L. Brown, Y.J. Chabal,
P.J. Szajowski, E.E. Chaban, L.E. Brus, and P.H. Citrin

November 1994

U. C. Lawrence Berkeley Laboratory
Library, Berkeley

FOR REFERENCE

Not to be taken from this room

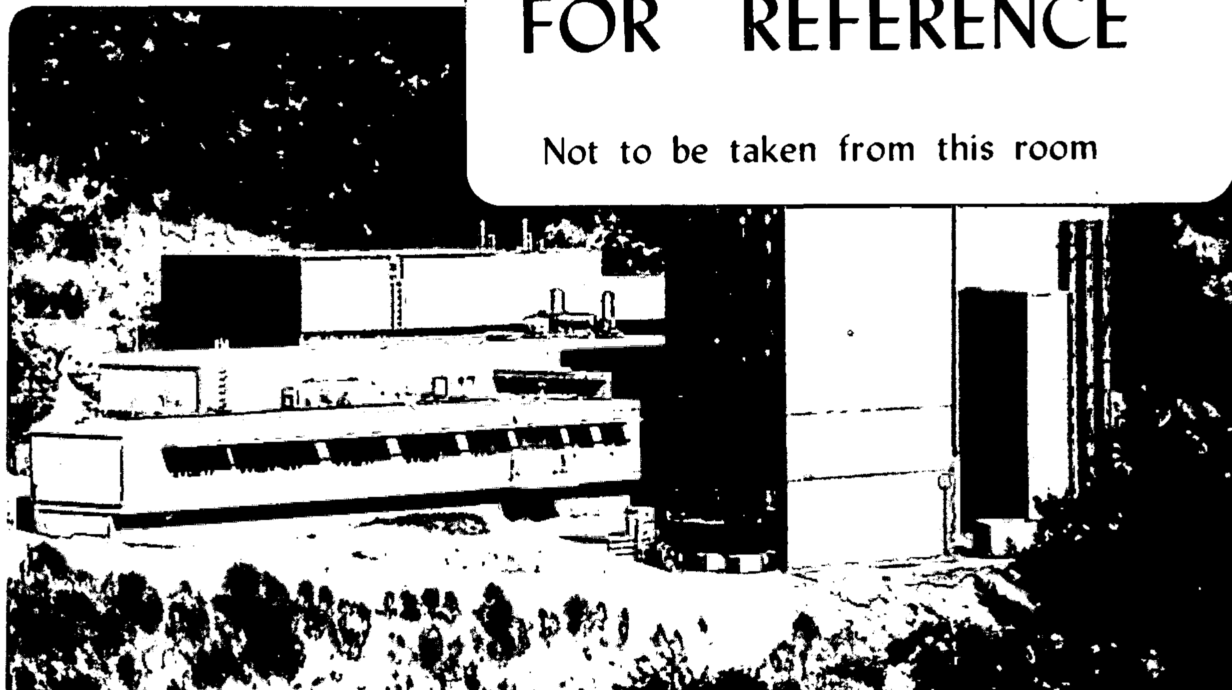

REFERENCE COPY | Does Not | Circulate | Bldg. 50 Library. | Copy 1 | LBL-36911

Prepared for the U.S. Department of Energy under Contract Number DE-AC03-76SF00098

DISCLAIMER

This document was prepared as an account of work sponsored by the United States Government. While this document is believed to contain correct information, neither the United States Government nor any agency thereof, nor the Regents of the University of California, nor any of their employees, makes any warranty, express or implied, or assumes any legal responsibility for the accuracy, completeness, or usefulness of any information, apparatus, product, or process disclosed, or represents that its use would not infringe privately owned rights. Reference herein to any specific commercial product, process, or service by its trade name, trademark, manufacturer, or otherwise, does not necessarily constitute or imply its endorsement, recommendation, or favoring by the United States Government or any agency thereof, or the Regents of the University of California. The views and opinions of authors expressed herein do not necessarily state or reflect those of the United States Government or any agency thereof or the Regents of the University of California.

LBL-36911

X-Ray Absorption Spectroscopy from H-Passivated Porous Si and Oxidized Si Nanocrystals

S. Schuppler, S.L. Friedman*, M.A. Marcus, D.L. Adler#, Y.-H. Xie, F.M. Ross†, T.D. Harris, W.L. Brown, Y.J. Chabal, P.J. Szajowski, E.E. Chaban, L.E. Brus and P.H. Citrin

AT&T Bell Laboratories
Murray Hill, NJ 07974

†Lawrence Berkeley Laboratory
Materials Sciences Division
National Center for Electron Microscopy
Berkeley, CA 94720

*Department of Applied Physics
Stanford University
Palo Alto, CA 90210

#Department of Materials Science
University of Illinois
Urbana-Champaign, IL 61801

Proc. MRS, Vol 375, (1995), in press

This work was supported by the Director, Office of Energy Research, Office of Basic Energy Sciences, Materials Science Division of the U.S. Department of Energy under Contract No. DE-AC03-76SF00098, financial support from the Alexander-von-Humboldt Foundation.

X-RAY ABSORPTION SPECTROSCOPY FROM H-PASSIVATED POROUS Si AND OXIDIZED Si NANOCRYSTALS

S. SCHUPPLER, S. L. FRIEDMAN,[a] M. A. MARCUS, D. L. ADLER,[b] Y.-H. XIE, F. M. ROSS,[†] T. D. HARRIS, W. L. BROWN, Y. J. CHABAL, P. J. SZAJOWSKI, E. E. CHABAN, L. E. BRUS, AND P. H. CITRIN

AT&T Bell Laboratories, Murray Hill, NJ 07974
[†]National Center for Electron Microscopy, Lawrence Berkeley Laboratory, Berkeley, CA 94720

ABSTRACT

Quantum confinement in nanoscale Si structures is widely believed to be responsible for the visible luminescence observed from anodically etched porous silicon (por-Si), but little is known about the actual size or shape of these structures. Extended x-ray absorption fine structure data from a wide variety of por-Si samples show significantly reduced average Si coordination numbers due to the sizable contribution of surface-coordinated H. (The H/Si ratios, as large as 1.2, were independently confirmed by ir-absorption and α-recoil measurements.) The Si coordinations imply very large surface/volume ratios, enabling the average Si structures to be identified as crystalline particles (not wires) whose dimensions are typically <15 Å. Comparison of the size-dependent peak luminescence energies with those of oxidized Si nanocrystals, whose shapes are known, shows remarkable agreement. Furthermore, near-edge x-ray absorption fine structure measurements of the nanocrystals shows the outer oxide and interfacial suboxide layers to be constant over a wide range of nanocrystal sizes. The combination of these results effectively rules out surface species as being responsible for the observed visible luminescence in por-Si, and strongly supports quantum confinement as the dominant mechanism occurring in Si particles which are substantially smaller than previously reported or proposed.

INTRODUCTION

The novel properties and possible utility of visible room-temperature luminescence from anodically-etched porous silicon (por-Si) have generated intense study [1]. Explaining the luminescence with quantum-confined structures has always seemed plausible [2,3], although it has not been possible to completely rule out alternative explanations. Until now, there have been difficulties in identifying the species responsible for the optical activity, along with determining its shape or dimensions, largely because the material is very inhomogeneous, but also because there is little direct structural information from the region lying within the penetration depth of the photoexciting radiation. Moreover, Si structures <20 Å, should they be significant, are beyond practical detection with standard methods such as electron microscopy.

This work summarizes recent x-ray absorption measurements [4] from a series of oxidized Si nanocrystals, whose shapes and sizes are known, and from a variety of anodically-etched (H-passivated) por-Si samples. The data, combined with luminescence emission measurements from each of the systems, establish considerably smaller values for the average size of Si structures contained within optically relevant depths of por-Si. Our conclusion are based not only on the strong correlation found between particle sizes and peak luminescence energies in the por-Si samples, but on the nearly identical correlation found for the Si nanocrystals.

Using our so-determined dimensions for the luminescent structures, however, leads to a large discrepancy with calculations of band gap versus size [5]. In the absence of defect-related states in the gap, the validity of a quantum-confinement model relies on a correspondence between band gap and luminescence energy. It is therefore important to know whether the lack of such correspondence for particles emitting in the visible region, i. e., <700 nm, lies with a problem in the theory or with the identification of the optically active species being Si rather than something else. In this regard, we present new results which demonstrate that the observed visible luminescence in the nanocrystals, and by extension in por-Si, is unrelated to an oxide-containing species.

EXPERIMENT

The Si *K*-edge absorption measurements were performed at the National Synchrotron Light Source using the AT&T X15B beamline [6] and InSb(111) monochromating crystals. Samples were kept at 77 K to minimize thermal disorder effects [7]. All data were obtained with total electron yield detection, whose effective sampling depth in 80%-porosity Si is < 2500 Å [8]. A variety of por-Si samples prepared under very different conditions [2,9-11] were studied with transmission electron microscopy (TEM), x-ray- and ir-absorption, α-recoil, and luminescence excitation and emission spectroscopies. Air exposure of the freshly prepared samples was limited to < 10 min in all but the TEM measurements to minimize O contamination (such effects are easily detectable). Samples of the O-passivated (air-insensitive) Si nanocrystals [12] were prepared for x-ray absorption measurements by transferring them as colloidal suspensions onto graphite substrates.

RESULTS

NEXAFS from Nanaocrystals

In Fig. 1 (a) we show Si *K* near-edge x-ray absorption fine structure (NEXAFS) data from three different sizes of oxidized Si nanocrystals, ox-Si_x, labelled small (*s*), medium (*m*), and large (*l*). A fourth sample containing even smaller nanocrystals and labelled very small (*vs*) was also measured. Its spectrum, omitted in Fig. 1(a) for clarity, appears in Fig. 2. Comparison with data from *c*-Si and bulk SiO_2 readily confirms that all the nanocrystalline samples contain crystalline silicon and SiO_2. The *c*-Si, SiO_2, and ox-Si_x data have been normalized to common "edge jump" values measured >100 eV above the Si *K* edge where their x-ray absorption intensities are structureless, i.e. , atomiclike.

Referring to Fig. 2, both the *m* and *vs* samples are composed mainly of *c*-Si and SiO_2. (Rather than using *c*-Si to model the Si in these samples, we have used a por-Si sample from Fig. 1(b), described below, whose NEXAFS more closely resembles that of the nanocrystals [13].) Closer inspection of the ox-Si_x spectra reveals additional structure between the absorption of *c*-Si and SiO_2. We can obtain an approximate spectrum for this species by subtracting the contributions from these two known components. The result is shown as a thin solid line (small artifactual structures near the *c*-Si and SiO_2 edges are due to imperfect modelling by the pure constituents).The intermediate energy position of its absorption edge leads naturally to the assignment of an incompletely oxidized Si species, SiO_x. Keeping in mind that x-ray diffraction, liquid chromatography, and TEM data [12] show the nanocrystals to be SiO_2-coated spheres of Si — whose outer diameters for the different samples are given in Table I — the assignment is entirely plausible: it just represents the interface layer between the crystalline core and the fully oxidized outer layer of the nanocrystals.

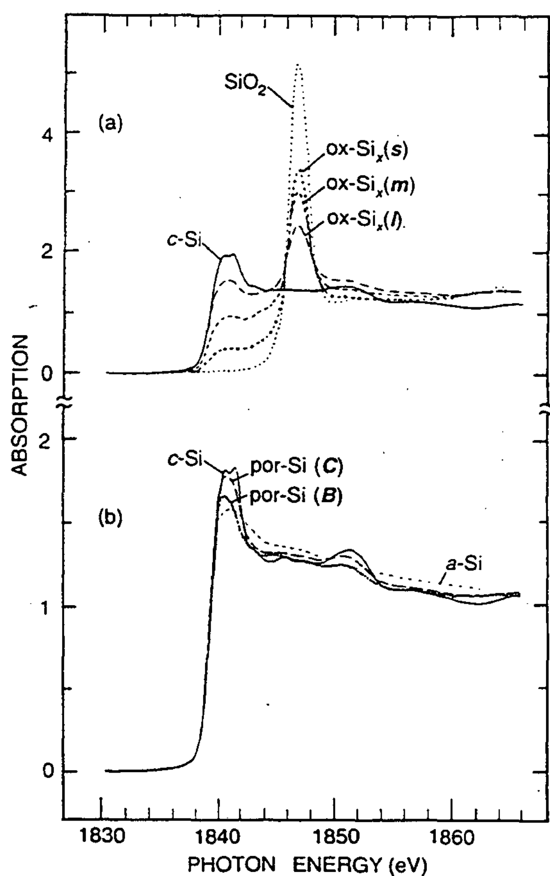

Fig. 1. (a) Si K-edge NEXAFS data from c-Si, SiO_2, and oxidized Si nanocrystals, labelled small (s), medium (m), and large (l). (b) NEXAFS data from c-Si, a-Si, and two different por-Si samples. All data in (a) and (b) are normalized to unity edge jump.

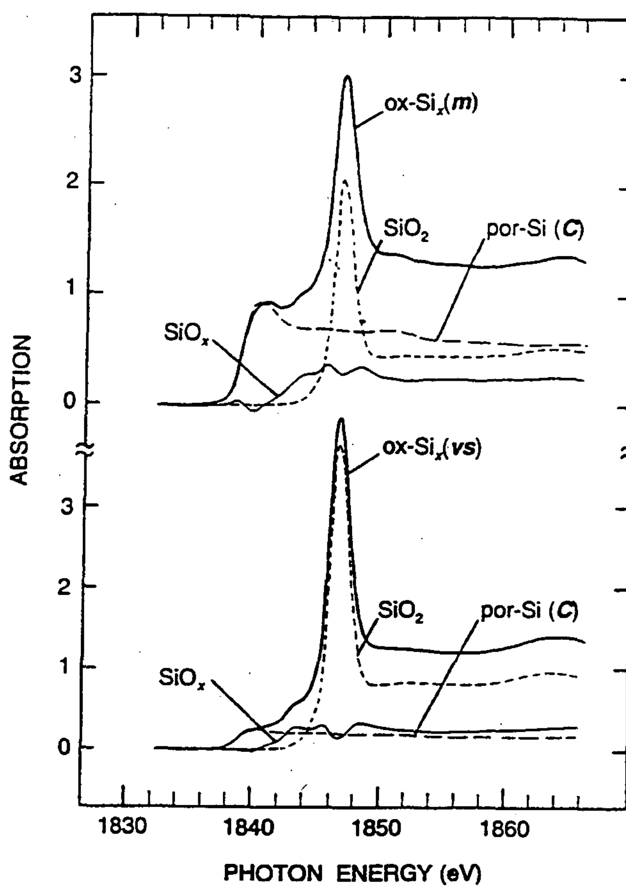

Fig. 2. Normalized NEXAFS data from medium (m) and very small (vs) oxidized Si nanocrystals, composed of Si inner core (here represented by por-Si(C) sample from Fig. 1(b)), SiO_2 outer shell, and interfacial sub-oxide shell SiO_x. Despite very different nanocrystal sizes, interfacial shell thicknesses and chemical compositions are the same.

Table I. Average dimensions of oxidized nanocrystals from TEM and NEXAFS data. D is diameter and t is layer thickness, in Å.

	D_{outer}	D_{middle}	D_{inner}	$t(SiO_x)$	$t(SiO_2)$
"very small"	26 ± 6	14	11	1.5	6
"small"	33 ± 6	21	17	2	6
"medium"	45 ± 7	34	31	1.5	5.5
"large"	96 ± 19	81	78	1.5	7.5

The relative mass fractions of the *c*-Si, SiO_2, and SiO_x contributions (i. e., their relative edge jumps) are converted into volume fractions using the corresponding densities [14]. From these volume fractions, the measured outer diameters [12], and the fact that the nanocrystals are spherical, we are then able to determine the mean inner diameters of the corresponding Si_x cores and the thicknesses of the intermediate SiO_x layer and the outer SiO_2 layer. The results are given in Table I [15]. Considering that for the four different samples the outer diameters vary by a factor of 4 and the inner diameters a factor of 7, it is remarkable that the thicknesses of both the intermediate SiO_x layer and the outer SiO_2 layer remain essentially constant. Furthermore, the SiO_x-layer thickness amounts to just about a monolayer, consistent with a very well-defined interface. Finally, the nearly indistinguishable edge position in the different nanocrystals, which directly reflects its chemical composition, indicates the absence of a size dependent change in interfacial stoichiometry.

The Si_x core diameters of the nanocrystals are plotted as circles in the bottom half of Fig. 3 versus their measured peak luminescence energies. The well-defined trend exhibits characteristics expected from a quantum-confinement picture: smaller particle sizes lead to higher emission energies. The constant thickness and stoichiometry of the interfacial suboxide layer, and the constant thickness of the outer SiO_2 layer found here for very different core diameters and peak luminescence energies effectively rule out SiO_x and SiO_2 as the optically active species, confirming quantum

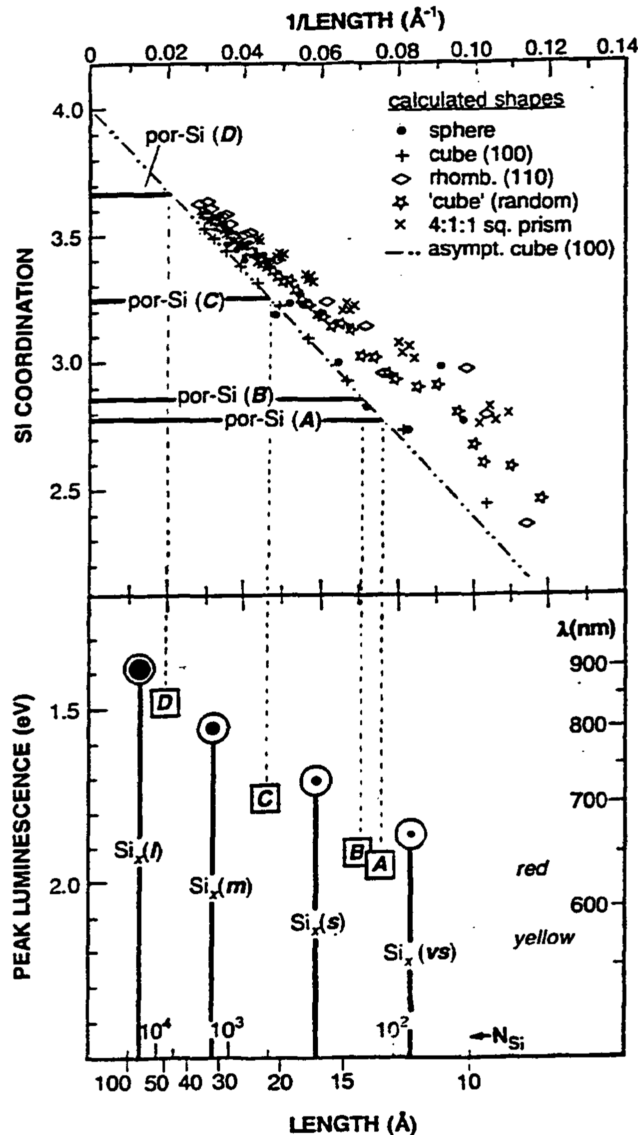

Fig. 3. *Top:* Correlation between average Si coordination for particles of different shapes versus their inverse characteristic length (diameter for sphere, side for cube). Average includes bulk and surface atoms, which have <4 first neighbors, explaining trend of lower values with decreasing particle size. Experimental Si coordinations from EXAFS data of four differently prepared por-Si samples labeled *A*, *B*, *C*, and *D* are indicated. *Bottom:* Correlation between average Si particle size and measured peak luminescence energy. Also indicated are total number of Si atoms, N_{Si}, contained in a cubic particle of corresponding size. Different sized oxidized Si nanocrystals labeled *vs*, *s*, *m*, and *l* are shown as circles, different por-Si structures from top figure are shown as squares.

confinement in the Si_x cores as being responsible for the observed luminescence from these systems. Recent high resolution luminescence data from such nanocrystals [16], in which vibronic structures associated with Si_x are observed, provide still additional support for this picture.

NEXAFS and EXAFS from Por-Si

Normalized NEXAFS data from por-Si appear in Fig. 1(b), along with comparison data from *c*-Si and *a*-Si. For clarity, we show only two of the four differently prepared samples studied here, labelled *C* [2] and *B* [10]. The qualitatively closer resemblance of the por-Si data to that of *c*-Si rather than *a*-Si, and the lack of (Si-O)-related absorption at ~1842 - 1848 eV, already noted elsewhere [10], are apparent.

While the NEXAFS data provide chemical information, i. e., electronic structure, the corresponding extended x-ray absorption fine structure (EXAFS) data readily provide local coordination and distance information, i. e., geometric structure [7]. In Fig. 4(a), we show the raw EXAFS data for the same samples displayed in Fig. 1(b). Locally ordered structure in the por-Si samples is seen from the second- and third-neighbor shells appearing as peaks at ~3.4 and 4.1 Å in

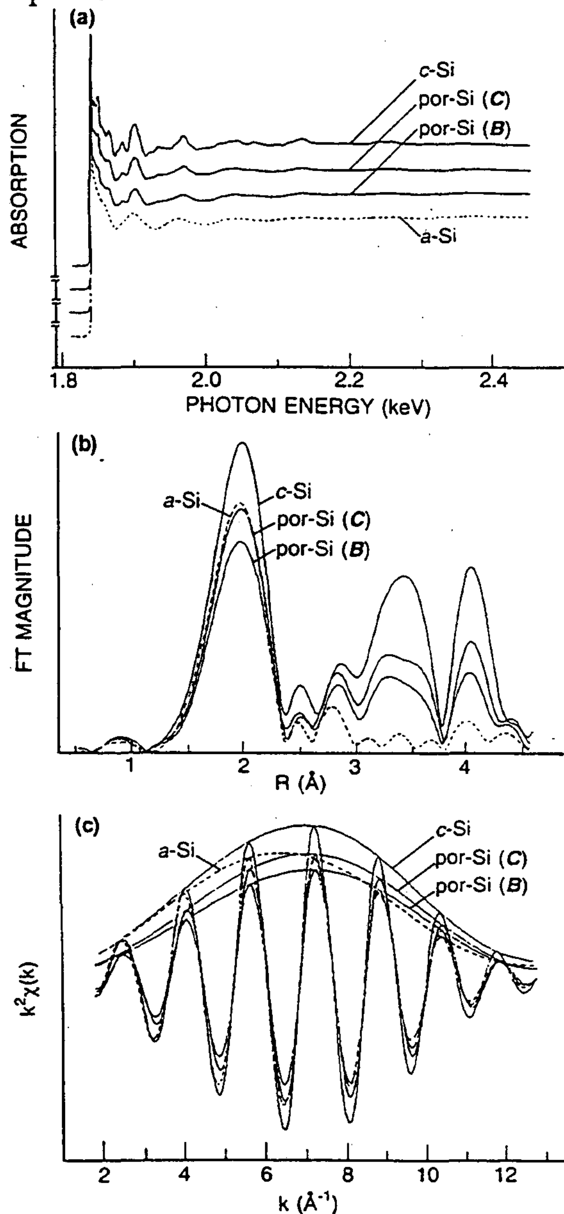

Fig. 4. (a) Raw Si *K*-edge EXAFS data from *c*-Si, *a*-Si, and two different por-Si samples. (b) Fourier transforms of edge-truncated, k^2-multiplied, background-subtracted data from samples in (a). 1st-, 2nd-, and 3rd-shell peaks at ~2.0, 3.4, and 4.1 Å are uncorrected for phase shift. Artifactual peaks at ~2.5 and 2.9 Å are due to truncation. (c) Back-transformed, filtered 1st-shell data from (b). Reduced EXAFS amplitudes from por-Si samples indicate lower Si coordination as a result of surface coordination to H. Measured average Si coordinations for different por-Si samples are plotted in Fig. 3.

the Fourier-transformed (FT) data [Fig. 4(b)]; such structure in *a*-Si is essentially absent, of course, due to static disorder. Relative to bulk *c*-Si, the apparently similar reduction of first-neighbor FT peak intensities at ~2.0 Å for the por-Si and *a*-Si samples is better understood by filtering and back-transforming the first-neighbor shells [Fig. 4(c)]. The peak intensity of the amplitude function $A(k)$, which envelopes the oscillatory EXAFS $\chi(k)$, is shifted for *a*-Si as a result of the Debye-Waller-like static-disorder term [7]. Such exponential damping of high-k scattering is unimportant for $k < 4$ Å^{-1}, so in that region $A(k)$ for the *a*-Si and *c*-Si samples is the same. This reflects their identical Si coordinations of 4. By contrast, $A(k)$ for the por-Si samples is *un*shifted relative to that for *c*-Si and is *smaller* at *all* values of k. This is an obvious indication that the average number of first-neighbor Si atoms, n_{Si}, in por-Si is <4.

The reason for the lower average Si coordination number and the apparent lack of other first neighbors in the FT data is that the surface Si atoms are also coordinated to H (the EXAFS backscattering amplitude of H is negligible). The substantially smaller values of n_{Si} obtained by fitting [7] the filtered por-Si data indicate large H/Si ratios in these samples. For example, $n_{Si} = 2.85 \pm 0.1$ in sample *B*, meaning H/Si = 1.15 ± 0.1, or an average H content of 115%. This should be compared with typical H concentrations of ~10% in device-quality *a*-Si:H [17]. Forward α-recoil measurements [14], which determine H/Si directly, give results for the corresponding por-Si samples that are completely consistent with those from EXAFS. Furthermore, these integrated H concentrations are confirmed by transmission ir-absorption measurements [18] (the ir results also show that H from bulk Si or from possible OH contamination is unimportant in the α-recoil data).

The large measured H/Si ratios imply large surface/volume ratios for the representative Si structures, the average sizes of which are determined in the top half of Fig. 3. We first plot calculated Si coordinations for different shapes as a function of inverse characteristic dimension, or length (i.e., diameter for a sphere, side for a cube). The dot-dashed line, drawn from the asymptotic limit of $n_{Si} = 4$ for infinitely large Si dimensions, is extended for (100)-faceted cubic particles of decreasing size. The 4:1:1 square-prism shapes are included to represent prolate particles. All particle surfaces (terminated with H) are ideal. To this calculated plot we then indicate the Si coordinations measured from the EXAFS amplitudes in the four different por-Si samples, labelled *A*, *B*, *C*, and *D* (all n_{Si} values are ± 0.1). Finally, the average Si particle sizes are obtained from the intersection of mean experimental Si coordinations with the asymptotic dot-dashed line. These sizes are plotted as squares in the bottom half of Fig. 3 against the peak luminescence energies measured in the corresponding samples. A correlation is obvious.

DISCUSSION

Before discussing the trend at the bottom of Fig. 3, we point out that the particle sizes represented by the squares are actually upper limits. The quoted particle sizes are obtained from the (100)-cubic asymptote, so any other assumed shape(s) would clearly lead to smaller sizes. Furthermore, TEM micrographs of the por-Si samples show them to contain *c*-Si, often in the form of columns, whose dimensions are ≥3 nm and whose amounts vary between 10 - 30% depending on the type of sample studied, e. g., *B* versus *C*. The remainder of the samples consists of Si structures too small to characterize with TEM. Since EXAFS measurements average over *all* the Si structures, including the contributions from *c*-Si, the reduced values quoted for n_{Si} — and thus the mass-weighted average particle sizes — would be even smaller had these larger *c*-Si contributions not been included. It is significant to note that subtracting the *c*-Si contributions from the por-Si data still leaves evidence for local crystallinity, i. e., the 2nd- and 3rd-neighbor shells in the FT data are not removed.

The bottom of Fig. 3 displays the important and surprising result that the relationship between peak luminescence energy and average particle size for the por-Si samples is nearly identical to that for the Si nanocrystals. Indeed, excluding the unetched *c*-Si contributions to our quoted n_{Si} values make the two trends virtually indistinguishable. The implication is clear: since the luminescence spectrum from a given Si particle is directly correlated with its size, the luminescence spectrum from a given por-Si sample is also associated with a characteristic Si dimension. Thus, for example, 720-nm peak luminescence from Si is representative of a structure whose average size is ~20 Å, *regardless of how the sample was prepared.*

The correlation in Fig. 3 also provides information about the shape of the Si species responsible for the luminescence in the *visible* region *<700 nm* (>1.75 eV). The columnar, extended-wire-like structures observed with TEM in por-Si samples *A* and *B* are all >20 Å, i. e., too large to account for our EXAFS results. If extended wire shapes were responsible for the luminescence in these samples, they would have to be of extremely small dimensions, <10 Å. This implies, therefore, that the optically active structures are generally not extended wires, but particles. We infer that these particles are predominantly (100)-faceted based on surface sensitive reflection ir-absorption measurements [19] from the por-Si *A* and *B* samples, which indicate H-Si frequencies representative of SiH_2 species [(110) or (111) surfaces would exhibit mainly SiH frequencies]. More general conclusions cannot be extended to samples luminescing in the near- and far-infrared region, i. e., >700 nm, because the distinction between wires and particles [see Fig. 3] is less significant.

The average sizes of the Si structures responsible for the *visible* luminescence in por-Si are small, well below easy detection with TEM or diffraction. For example, Fig.3 indicates that 2-eV luminescence is associated with particles of dimensions typically less than 13 Å (recall that the values shown in squares are upper limits). This is considerably smaller than any size previously associated with such luminescence. A 13-Å cube contains a total number of Si atoms $n_{Si} \approx 110$ ($\approx$ 60 for a sphere [20], see Fig. 3) and a calculated band gap of ~3.8 eV [5], whereas a 26-Å cube has corresponding numbers of ~900 and 2.2 eV. Factors of two in size are therefore very important.

Basic questions about visible photoluminescence from por-Si still remain. Among the most important of these is a reliable calculation of the coulombic interaction between electrons and holes localized on a Si particle. A complete description of the visible-luminescence mechanism in por-Si will ultimately need to address this and other issues, along with the fact that the optically active Si species in this material has dimensions as small as those found here.

ACKNOWLEDGEMENTS

S. Schuppler is grateful to the Alexander-von-Humboldt Foundation for financial support. The EXAFS experiments were performed at the NSLS, Brookhaven National Laboratory, which is supported by the DOE, Division of Materials Sciences and Division of Chemical Sciences. The TEM measurements, performed at the National Center for Electron Microscopy, LBL, are supported by the Director, Office of Basic Energy Sciences, DOE, under contract number DEAC03-76SF00098.

REFERENCES

[a] Present address: Department of Applied Physics, Stanford University, Palo Alto, CA 90210.
[b] Present address: Department of Materials Science, University of Illinois, Urbana-Champaign, IL 61801.

1. For example, see Mater. Res. Soc. Proc. **256** (1992); **283** (1993); **298** (1993).

2. L. T. Canham, Appl. Phys. Lett. **57**, 1046 (1990)
3. V. Lehmann and U. Gösele, Appl. Phys. Lett. **58**, 856 (1991)
4. S. Schuppler, S. L. Friedman, M. A. Marcus, D. L. Adler, Y.-H. Xie, F. M. Ross, T. D. Harris, W. L. Brown, Y. J. Chabal, L. E. Brus, and P. H. Citrin, Phys. Rev. Lett. **72**, 2648 (1994).
5. See, e. g., C. Delerue, G. Allan, and M. Lannoo, Phys. Rev. B **48**, 11024 (1993), and references therein.
6. A. A. MacDowell, T. Hashizume, and P. H. Citrin, Rev. Sci. Instr. **60**, 1901 (1989).
7. P. A. Lee, P. H. Citrin, P. Eisenberger, and B. M. Kincaid, Rev. Mod. Phys. **53**, 769 (1981).
8. A. Erbil, G. S. Cargill, R. Frahm, and R. F. Boehme, Phys. Rev. B **37**, 2450 (1988). Escape depths have been crudely estimated by multiplying by 5 to account for the 80% porosity.
9. Preparations of the por-Si samples studied here (referred to as *A, B, C,* and *D*) follow those in Refs. 2, 10, and 11, namely, *C* [2]: *p*-type Si(100), >50 Ω-cm, 20%HF in alcohol, 20 mA/cm^2 for 5 min; *A* [11]: same as *C*, but etched 60 min; *B* [10]: *p*-type Si(100), >50 Ω-cm, 15%HF in alcohol, 25 mA/cm^2 for 12 min; *D* [11]: *p*-type Si(100), 0.5-0.8 Ω-cm, 40% HF in alcohol, 50 mA/cm^2 for 80 sec, soaked 2 hr unetched in same solution.
10. S. L. Friedman, M. A. Marcus, D. L. Adler, Y.-H. Xie, T. D. Harris, and P. H. Citrin, Appl. Phys. Lett. **62**, 1934 (1993).
11. Y. H. Xie, M. S. Hybertsen, W. L. Wilson, S. A. Ipri, G. E. Carver, W. L. Brown, E. Dons, B. E. Weir, A. R.Kortan, G. P. Watson, and A. J. Liddle , Phys. Rev. B **49**, 5386 (1994); Y.-H. Xie (unpublished).
12. Oxidized Si nanocrystals were made by homogeneous nucleation in high-pressure He at 1000°C from thermal decomposition of disilane with subsequent oxidation in O_2 at 1000°C for ~30 msec. See K. A. Littau, P. J. Szajowski, A. J. Muller, A. R. Kortan, and L. E. Brus, J. Phys. Chem. **97**, 122 (1993); W. L. Wilson, P. J. Szajowski, and L. E. Brus, Science **262**, 1242 (1993); P. J. Szajowski and L. E. Brus (unpublished).
13. Like the nanocrystals, the por-Si sample also consists of small particles whose band structure is not fully developed, and therefore exhibits neither the larger white-line to edge-jump ratio nor the split white-line structure of *c*-Si. Our results are completely unaffected by this choice because only difference spectra are being compared.
14. Densities and molecular weights for bulk *c*-Si , SiO_2, and SiO were used, i. e., 2.33, 2.4, and 2.1 gm cm^{-3}, respectively.
15. It should be noted that while the outer diameters of the nanocrystals, determined by TEM in Ref. 12, have very conservative error limits of ≤20 %, the relative mass fractions, determined by NEXAFS, are much more precise. Thus, the relative error limits of the inner diameters and the oxide layer thicknesses are just the same as for the outer diameters.
16. L. E. Brus, P. F. Szajowski, W. L. Wilson, T. D. Harris, S. Schuppler, and P. H. Citrin, J. Amer. Chem. Soc. (to be published).
17. R. A. Street, *Hydrogenated Amorphous Silicon* (Cambridge University Press, Cambridge, 1991).
18. The volumes used for integrating the measured SiH_x concentrations in the por-Si samples were obtained from TEM.
19. Surface sensitivity of <1μm was obtained using a grazing internal incidence angle in a Ge plate positioned next to the por-Si samples.
20. For a Si cube of side *L*, $N_{Si} = 8L^3/a_0^3$; for a sphere of diameter *L*, $N_{Si}^{sph} = (\pi/6)N_{Si}^{cube}$.

LAWRENCE BERKELEY LABORATORY
UNIVERSITY OF CALIFORNIA
TECHNICAL INFORMATION DEPARTMENT
BERKELEY, CALIFORNIA 94720